INTERNATIONAL JOURNAL OF NOVEL RESEARCH AND DEVELOPMENT (IJNRD)
© 2026 IJNRD | Volume 11, Issue 2, February 2026 | ISSN: 2456-4184 | IJNRD.ORG

ENHANCED LIVER TUMOUR SEGMENTATION USING CONTEXTUAL VISION UNLEASHED

[1]Anjana V T, [2]Dr. Tajunisha N

[1]Ph.D Research Scholar, [2]Professor
[1] Department of Computer Science,
[1] Sri Ramakrishna College of Arts and Science for Women, Coimbatore, Tamil Nadu, India

Abstract: Identifying and segmenting liver tumours automatically using medical imaging modalities such as CT scans to allow for early cancer detection and treatment planning is necessary, yet complicated by factors such as noise in the image acquisition and heterogeneous boundaries of the tumours. To improve prior work in this area, this paper proposes a two-stage integration approach to successively denoise the CT image first, then segment the liver tumour. In this manner, this method addresses the cause of segmentation failures caused by prior imaging issues. The first stage of the proposed Spectra Vision Vortex Denoiser (SVVD) is validated containment of artefacts while restoring or preserving, the structural integrity of liver tissue, and yielding a higher PSNR and SSIM scores compared to other imaging denoising techniques. The Contextual Vision Unleashed (CVU) Segmentation Algorithm is then applied to the clean image from the denoising. With this approach, segmentation is performed with respect to local intensity and structure patterns through adaptive thresholding and morphological operations to delineate tumour boundaries. This method lessens problems of over segmentation and dependence on noise. The performance evaluation shows substantial increases in DSC, IoU, and Pixel Accuracy, confirming that this framework is a robust and reliable tool for clinically detecting liver tumours.

***Keywords*: Adaptive Thresholding, Denoising Image Segmentation, Liver Tumour, Morphological Operations, Structural Similarity**

1. INTRODUCTION

Detecting and segmenting liver tumours are important for early diagnosis and treatment planning and ultimately improving the patients' survival rate with hepatic malignancies. With medical imaging advances, particularly with CT and MRI imaging modalities, deep learning based techniques have improved localising and classifying tumours. The complexity of the liver structures and the potential for differences in appearance of the tumours has been an obstacle for automated analysis.

The Liver Tumour Segmentation Benchmark (LiTS) created a convenient webpage to compare liver tumour segmentation methods, facilitating researchers to compare models in a large-scale segment [1]. It was on this that a deep learning-based ResUNet model has been proposed to segment the liver and tumour areas in CT images with accuracy and lower computational time [2]. Furthermore, discriminative features and supervised learning functions that can be obtained have also been shown to successfully predict tumour parameters [3].

There are recent studies that have explored fluorescence imaging with 5-aminolevulinic acid (ALA) for improved instant visual performance of the tumour, which surgeon can see better in surgery [4]. Similarly, brain tumour detection has been conducted using data augmentation and convolutional neural networks (CNNs) showing that deep learning can be effective even with very small datasets [5]. Likewise, a large-scale deep-learning architecture has shown good accuracy in multi-class brain tumour classification [6].

Hybrid deep learning frameworks of LeU-Net have been effectively used to segment brain tumours using 2D MRI as well to enhance structural knowledge about the tumour regions [7]. The biomarker research found out that Alpha-Fetoprotein (AFP) and its forms are important tumour recurrence predictors in patients with hepatocellular carcinoma [8]. CNN and SVM based threshold segmentation combination further increased the accuracy of the MRI-based tumour classification [9].
The next steps, such as Eres-UNet++, which implemented channel attention mechanism, were shown to perform better on liver CT image segmentation tasks [10]. New biomarkers like serine protease inhibitor kazal have been suggested in the detection of hepatocellular carcinoma in patients with metabolic liver diseases [11]. MRI liver-portal vein contrast ratios have also been used to analyze quantitatively in order to increase the diagnostic thresholds used to diagnose hepatobiliary abnormalities [12].
Deep learning models such as sine-cosine fitness grey wolf optimization, which are optimized, have improved accuracy in brain tumour classification [13]. Deep learning models are also used in contrast-enhanced ultrasound imaging with automatic lesion classification of the liver, which is an efficient diagnostic aid [14]. Radiometrics methods have also shown the potential in forecasting the development of new hepatocellular carcinoma among high-risk cirrhosis patients using CT scans [15].
In addition, the digital pathology and machine learning have transformed the analysis of liver, kidney, illnesses, and made it possible to make the analysis of cross-organ diagnosis predictions more precise [16]. An intra-operative blood salvage samples study revealed the presence of tumour cell using the latest microfluidic technology, which led to the safer liver transplantation operations [17]. Recent changes in clinical practice underline the importance of non-invasive biomarkers in the assessment and management of nonalcoholic fatty liver disease, ensuring the creation of diagnostic paths that patients can follow [18].
Recent studies have demonstrated that hybrid structures based on the E-UNet, such as Rdctrans E-Unet and -U-Net, that incorporate structural learning or ensemble learning, are very promising for segmenting liver CT images [19]. Additionally, this provides

additional rationale for colorectal cancer screening, especially in low-income, rural, and minority populations. Interestingly, the significant number of people with non-invasive colorectal cancer cannot be understated in the interactions that occur in these populations[20].

2. BACKGROUND STUDY

Wullareth et al. (2023) [20] studied ctDNA as a liver metastases biomarker of colorectal cancer, and concluded that it is a highly useful biomarker in treatment planning and monitoring cancer.

A 10-year retrospective study conducted by Rola et al. (2022) [21] on liver surveillance in patients with uveal melanoma indicated that imaging surveillance is still essential, as the markers have proven to be helpful in the detection of initial liver metastasis.

Zhuo et al. (2022) [22] took advantage of collagen-predegrading glypican-3-targeting imaging of the hepatocellular carcinoma in fibrotic liver, and enhanced its visualization of the tumour and the overall diagnostic capacity. In [23], Bin et al. investigated the importance of H2 calponin antigen and autoantibodies as a method of improving the immune-based diagnostics of liver cancer metastasis.

Ou et al. (2024) [24] argue that GPRC5A has been identified to mediate liver metastasis and resistance to drugs in breast cancer via the mTOR signaling pathway [24], which represents a molecular marker that can be used to treat the disease.

Chalasani et al. (2022) [25] established that a blood test, a multi-target blood test, had high sensitivity in early detection of hepatocellular carcinoma, which understand as a positive move in a noninvasive diagnostic screening test.

Turner et al. [26] synthesized a near-infrared anti-MUC5AC probe enabling selectivity of pancreatic cancer metastases in the liver, thereby proving its contribution to individual oncology. Graphene-based biosensors and their derivatives are reviewed by Pourmadadi et al. [27] because of their important electrical sensitivity, these devices can detect cancerous cells quickly and accurately.

Tang et al. (2023) [28] designed a hypoxia-responsive photosensitizer that targeted organelles and organelle-ores enhanced the outcome of photodynamic therapy in solid tumours in the liver and other areas. Peneau et al. (2021) [29] examined the genomics of liver tumours related to viral hepatitis and revealed novel significant molecular pathways essential in the process of hepatocarcinogenesis.

Alshagathrh and Househ (2022) [32] conducted a systematic review of techniques used to identify indicators of fatty liver in the ultrasound image that eg. explain the techniques used to determine the amount of liver fat to predict early liver disease diagnosis.

Table 1. Literature Research on the New Studies about Liver Tumour Detection and Analysis.

Ref. No.	Author(s)	Year	Area of Focus	Methods & Methodologies	Limitations
[33]	Tang et al.	2023	Hypoxia-responsive photodynamic tumour therapy	Developed a dual-organelle-targeting photosensitizer responsive to hypoxic tumour environments to enhance photodynamic therapy (PDT) efficacy.	Requires precise control of oxygen levels; limited validation on large-scale in vivo tumour models.
[34]	Li et al.	2022	Liver tumour progression and intestinal disruption	Used xmrk oncogene transgenic zebrafish model to study how liver tumour progression affects intestinal structure and molecular pathways.	Findings based on animal models; human clinical translation not fully validated.
[35]	Kim et al.	2021	Liver cancer segmentation benchmark	Organized PAIP 2019 Liver Cancer Segmentation Challenge using histopathological WSIs with standardized metrics for deep learning model evaluation.	Limited dataset diversity; focus restricted to histopathology images, not multimodal scans.
[36]	Kim et al.	2021	Liver cancer segmentation benchmark (duplicate study)	Similar to [35]; provided annotated datasets and benchmark results for segmentation tasks.	Redundant reference; same limitations as [35].
[37]	Das et al.	2023	Biomarkers in cancer detection and diagnosis	Reviewed advanced biosensing and molecular biomarker techniques for early cancer diagnosis and prognosis assessment.	Lacks computational integration; does not explore deep learning-based biomarker fusion or automation.

Contribution: have created and tested a two-step framework of a liver tumour analysis in this work. used the Spectra Vision Vortex Denoiser to sharpen images without altering the structural information and used the Contextual Visual Unleashed (CVU) Segmentation Algorithm to reliably and accurately label tumours. The suggested methodology was more effective compared to the methods previously established based on the number of key performance indicators; therefore, a feasible and strong step towards improvement of clinical diagnostic practices.

Organization: The paper is written in five parts. Section 1 provides the significance of analyzing liver tumours and drawbacks of the means. In this section 2, the earlier sections are reviewed and limitations in the earlier sections are pointed. In section 3, the proposed method is discussed and the Spectra Vision Vortex Denoiser and the CVU Segmentation Algorithm are described. Section 4 explains the experiment, metrics applied to assess findings and presents comparative findings. Lastly, the main findings and recommendations to future work are provided in Section 5.

3. PROPOSED METHODOLOGY

A. Dataset
Dataset: https://www.kaggle.com/datasets/harshwardhanbhangale/lits-dataset

The list dataset on Kaggle is a big set of liver CT images that were developed to undertake the segmentation and analysis task. It consists of 58,638 pictures, and the total amount of data is approximately 2 GB, which means that there is enough information to conduct the training and testing of liver tumour detection models. The size of the images is equal, 256 × 256 pixels, and they can be processed by tools of deep learning easily. The dataset is diverse in terms of liver tissue and tumour variations and is useful in making models learn to tackle various cases. It has been extensively applied as a standard to compare the accuracy and efficiency of liver tumour segmentation and denoising algorithms.

The suggested methodology will be used to improve the liver CT images with the help of state of-the-art denoising and segmentation methods. The Spectra Vision Vortex Denoiser is initially used to de-noise the image while maintaining important structural information of the liver and tumour area to produce high-quality images that can be processed further. Later on, the Contextual Vision Unleashed (CVU) Segmentation Algorithm is used to determine liver tumour boundaries using adaptive thresholding and morphological operations. Such a combination methodology can solve the shortcomings of the current methodologies, including noise sensitivity, excessive segmentation, and lack of edge preservation, to deliver high-quality and accurate segmented images. The metrics applied in performance evaluation (MSE and PSNR and SSIM to denoising and DSC, IOU, sensitivity, specificity, and pixel accuracy to segmentation) are used to guarantee thorough evaluation.
Figure 1 This is the overall architecture that depicts a medical image processing architecture that processes liver tumours in two stages Denoising and Segmentation and Evaluation. The input liver CT image has then initiated the proposed process whereby the image is first sent to the Proposed Denoising Algorithm (Spectra Vision Vortex Denoising) to remove noise and bring a selected image with a higher diagnostic visibility. This is further inputted into the Proposed Segmentation Algorithm (Contextual Vision Unleashed -CVU Segmentation) and this is then used to isolate and outline the region of the liver tumour more accurately and it provides results of the Masked Tumour, Contour Map and Segmentation Overlay. Lastly, the Evaluation Stage is a quantitative assessment of all the performances of all the modules, where the MSE, PSNR, SSIM, Accuracy, will be computed in the denoising step, Dice Similarity Coefficient (DSC), Intersection over Union (IoU), will be computed in the segmentation. The graphical plotting of results is stored to be further analysed in future and this gives a keen evaluation of the proposed liver tumour detector pipeline.

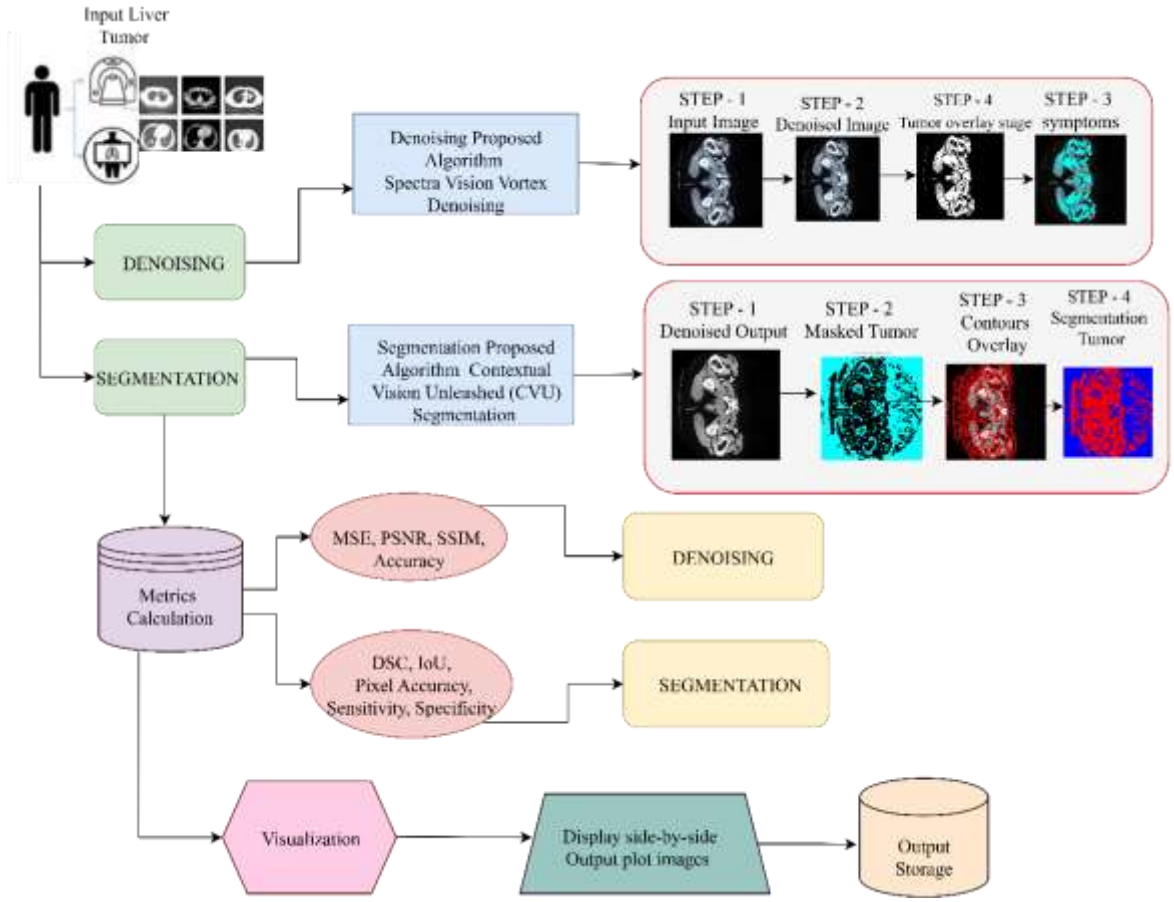

Figure 1: Denoising and Segmentation Architecture for liver tumour.

B. Spectra Vision Vortex Denoise Algorithm Proposal.

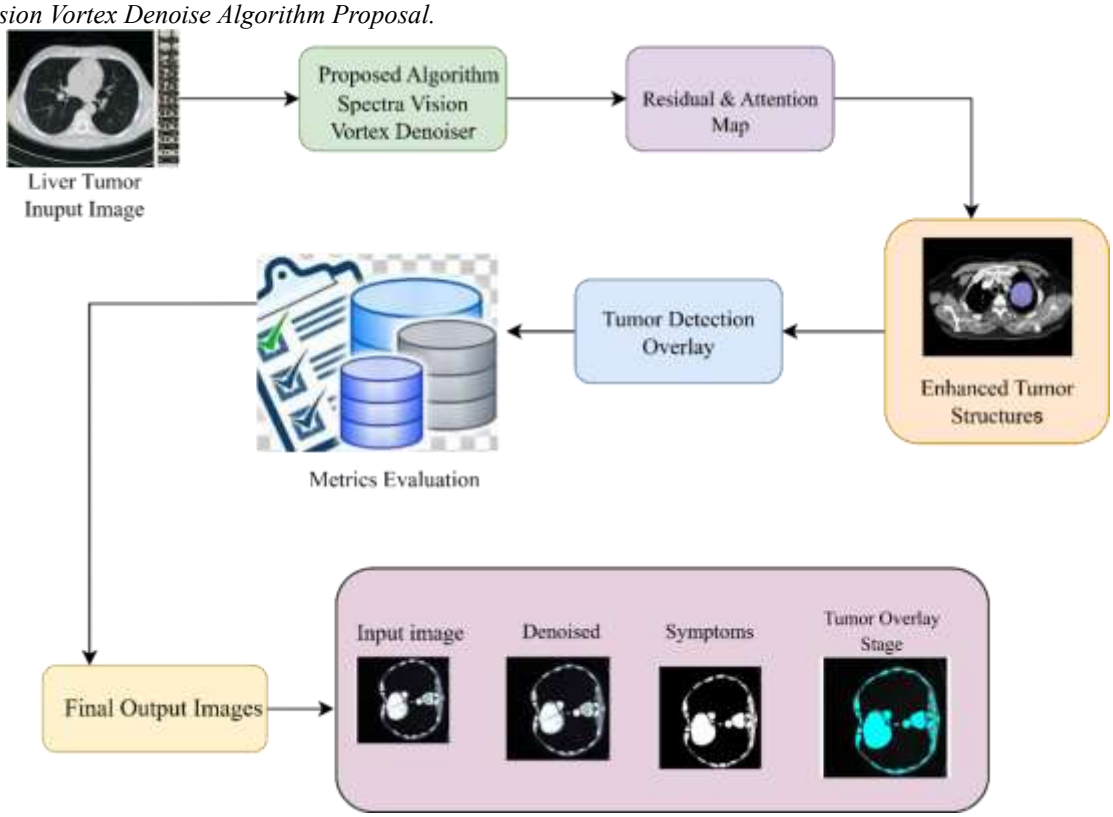

Figure 2: Denoising Using Spectra Vision Vortex Denoiser

Figure 2 can be used to show the denoising architecture which is designed to advance and detect liver tumours in computed tomography (CT) images, and the Spectra Vision Vortex Denoiser framework was created to do so. The input of the process is the liver CT image that is processed by the proposed algorithm named Spectra Vision Vortex Denoiser to create Residual and Attention Map. The map is used to increase the high-frequency details of the images especially the tumour boundaries and the spatially important regions of the liver. The Residual and Attention Map combination enhances the structure of liver, leading to a sharper, denoised image which was then further sent to Tumour Detection Overlay module to locate it accurately. To test the effectiveness of the framework, Metrics Evaluation stage is used that evaluates quality of the images and accuracy of the segmentation. The last sequence provides better visualization results, which show the original liver CT image, the denoised output, the symptom mask and the final tumour overlay to be interpreted by the clinician.

Step 1: Input Image Acquisition

The raw image is represented as:

$I(x, y)$ ---------- (1)

In Equation (1),I intensity value at pixel coordinates, x, y spatial coordinates of the image. This stands the intensity values of the raw input image at every pixel. It provides the original image data for denoising and serves as the starting point for all processing.

Step 2: Vortex-Based Filtering

Vortex filtering emphasises structural features while reducing random noise.

$I_v(x, y) = I(x, y) * V(x, y)$ ---------- (2)

In Equation (2), $I_v(x, y)$ image after vortex-based filtering, $I(x, y)$ input image,$*$ convolution operation, $V(x, y)$ vortex filter kernel, designed to preserve edges and smooth noise. Convolution with a vortex filter emphasises edges and structural details while reducing random noise. It prepares the image for spectral analysis.

Step 3: Spectral Frequency Transformation

Transform the filtered image to the frequency domain using the 2D Fourier Transform:

$F(u, v) = \mathcal{F}\{I_v(x, y)\}$ ---------- (3)

In Equation (3), $F(u, v)$ frequency domain representation of the image, u, v frequency domain coordinates, $\mathcal{F}$ 2D Fourier Transform operator. The filtered image is transformed to the frequency domain to separate noise (high-frequency componentsfrom the underlying structural information of the image.

Step 4: Adaptive Spectral Filtering

Suppress noise in the frequency domain with an adaptive filter:

$F_{denoised}(u, v) = F(u, v).H(u, v)$, $H(u, v) = \frac{(|F(u,v)^2}{|F(u,v)|^2 + \sigma_n^2}$ ---------- (4)

In Equation (4),$F_{denoised}(, v)$ spectrally filtered (denoised) image in the frequency domain $H(u, v)$ adaptive spectral filter,$(|F(u, v)^2$ power spectrum of the image. σ_n^2 estimated noise variance. Selective noise suppression in the frequency domain reduces high-frequency noise while retaining important structural information.

Step 5: Inverse Fourier Transform

Return the denoised image to the spatial domain:

$I_{denoised}(x, y) = \mathcal{F}^{-1}\{\mathcal{F}_{denoised}(u, v)\}$ ---------- (5)

In Equation (5), $I_{denoised}(x, y)$ spatially filtered image in the spatial domain.$\mathcal{F}^{-1}$ inverse 2D Fourier Transform. Transforms the denoised image back to the spatial domain for further refinement or visualisation.

Step 6: Vortex Motion Modelling & Spectral Attention (Refinement)
Further refinement enhances edges and suppresses residual noise:
$I_{final}(x,y) = I_{denoised}(x,y) + \alpha . W_v(x,y) . \nabla I_{denoised}(x,y)$ ---------- (6)
In Equation (6), $I_{final}(x,y)$ final denoised image.α weighting factor controlling the amount of refinement.$W_v(x,y)$ vortex motion attention map, highlighting areas requiring edge preservation.$\nabla I_{denoised}(x,y)$ sssgradient of the denoised image (edge information). Refines edges and further suppresses residual noise using vortex motion attention.

Algorithm: Spectra Vision Vortex Denoiser
Input: I(x, y) 1. Normalise the image: I_norm = I / 255.0 2. Compute residual to capture high-frequency details: Residual = I_norm - Blur(I_norm, kernel_size=3x3) 3. Compute the attention map based on residual: Attention = Gaussian Blur(abs(Residual), kernel_size=5x5) 4. Enhance image using residual and attention: Enhanced = I_norm + Residual * (1 + Attention) 5. Clip values to the valid range [0, 1]: Enhanced = Clip(Enhanced, 0, 1) 6. Convert back to an 8-bit image: I_denoised = Enhanced * 255 7. Return I_denoised Output: I_denoised(x, y)

The input image is normalised by use of pseudocodes and then residual is calculated by getting the difference between the blurred image and the result is obtained which amplifies the noise and fine details within the residual image. The residual image produces an attention map through a Gaussian blur to allow the important areas to stand out. The combination of the residual and attention gives us the image desire since all do is to add the two to get the image want to suppress noise and enhance edges. The output is clipped in such a way that no pixels are out of range and transformed to produce an 8-bit image which is now in the desired denoised output.

C. Proposed Contextual Vision Unleashed (CVU) Segmentation Algorithm for Liver Tumour Detection
Contextual Vision Unleashed (CVU) Segmentation Algorithm is a segmentation algorithm that uses adaptive thresholding and morphological operations to effectively segment liver tumour in medical images. The input is the denoised liver image of the Spectra Vision Vortex Denoiser which makes sure that the segmentation is done on a clean and noise free image to achieve high accuracy. The analysis of local intensity changes and local structure patterns is conducted to outline the boundaries of the tumour. Previously used forms of segmentation had limitations of over-segmentation, noise sensitivity and poor boundary resolution which undermined the identification of tumours. The proposed CVU Segmentation Algorithm is an enhancement of these algorithms because it combines the local adaptive analysis with structural refinement in order to promote local adaptive analysis with clearly defined tumour regions without compromising edges and minimizing artefacts. This method is more accurate and specific in liver tumour segmentation giving the best possible output in the segmentation of liver tumours.

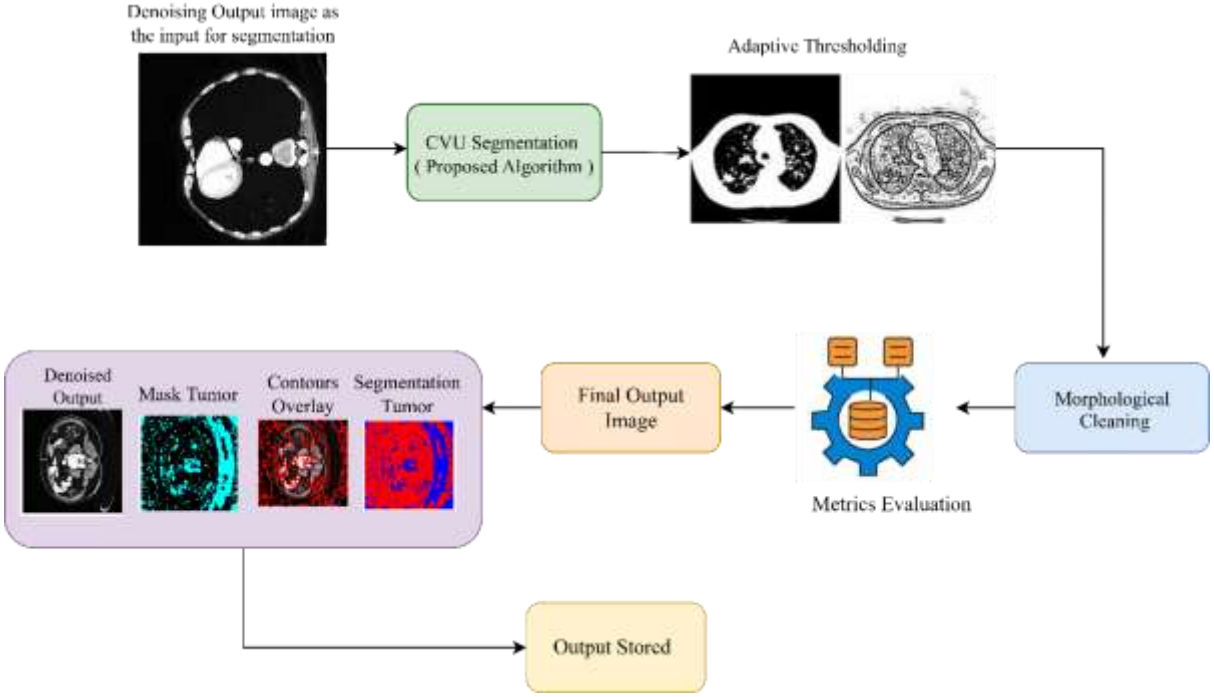

Figure 3: Segmentation Using Contextual Vision Unleashed
In Figure 3 , The segmentation architecture depicts a tumour segmentation algorithm, which has a liver CT image as input and the algorithm goes through CVU Segmentation algorithm, which isolates the liver parts and gives a segmented mask. The resulting output is then processed through a number of post-processing processes as illustrated in the Denoised Output subsection, such as the

formation of Final Mask Tumour, Contours Overlay, and Segmentation Tumour images. The next step is called the Morphological Cleaning step which cleans the mask by eliminating noise and softening the edges. The Final Output Image of the cleansed mask is stored to be analysed later and to store the liver tumours.

Step 1: Input Image Preparation

$I_{denoised}(x, y)$ ---------- (7)

In Equation (7), $I_{denoised}$ Denoised input image at pixel x, y. Pixel coordinates x, y.This is the denoised liver image obtained from the Spectra Vision Vortex Denoiser. It serves as the starting point for segmentation. Each pixel x, yContains an intensity value representing liver tissue after noise removal processing occurs, yet this image is clean and ready for segmentation.

Step 2: Adaptive Thresholding

$$T(x, y) = mean\big(I_{local}(x, y)\big) - C$$

$S(x, y) = \{^{255,\ if(I_{local}(x,y))>T(x,y)}_{0,\ \ otherwise}$ ---------- (8)

In Equation (8), A local window around each pixel is considered ($I_{local}(x, y)$,and its mean intensity is calculated. A constant $C$is subtracted to fine-tune sensitivity. Pixels above $T(x, y)$are are classified as tumours (255), others as background (0). Local adaptive thresholding separates potential liver tumour regions from the background based on neighbourhood intensity values.

Step 3: Morphological Operations

$$S_{open} = S \circ K$$

$S_{close} = S_{open} \cdot K$ ---------- (9)

In Equation (9), Opening **(**$\circ$**)** , erosion followed by dilation removes tiny isolated pixels (noise). Closing **(**$\cdot$**)** Dilation followed by erosion fills small holes inside tumour regions. $K$is, the structuring element used for morphological processing. Morphological processing improves the binary mask, removing small noise and filling gaps in tumour regions.

Step 4: Output Tumour Mask

$S_{final}(x, y) = S_{close}(x, y)$ ---------- (10)

In Equation (10), $S_{final}(x, y)$ Final liver tumour segmentation mask.x, y Pixel coordinates. The final segmented mask identifies liver tumour regions clearly and is ready for visualisation, overlay, or quantitative analysis. Combines results from thresholding and morphological refinement. Tumour pixels are 255, background pixels are 0, producing a clean binary map.

Algorithm 2: Contextual Vision Unleashed

```
Input: I_denoise(x, y)
Step 1: Input Image Preparation
   - Load I_denoise(x, y)
   - Each pixel holds an intensity value after denoising
Step 2: Adaptive Thresholding
   For each pixel (x, y):
      - Compute local mean: mean_local = mean(I_denoise in neighborhood)
      - Compute threshold: T(x, y) = mean_local - C
      - Generate initial mask:
         If I_denoise(x, y) > T(x, y):
            S(x, y) = 255   // Tumour
         Else:
            S(x, y) = 0
Step 3: Morphological Refinement
   - Define structuring element K (e.g., 3x3 square)
   - Apply opening: S_open = S ∘ K       // Remove small noise
   - Apply closing: S_close = S_open • K  // Fill small holes

Step 4: Output Tumour Mask
   - S_final(x, y) = S_close
   - Return S_final(x, y) as the segmented liver tumour mask
Output: S_final(x, y)   // Final segmented liver tumour mask
```

In the given pseudocode, the liver image after cleaning is then considered as input and the local adaptive threshold is set on each pixel and then used to identify the regions of tumours and the background. This is continued by calculation of the initial binary mask where any pixel above adaptive threshold is taken as one of the possible tumours. Two structural cleanup transformations are then applied on this mask, to remove minor quantities of clean spurious pixels and fully missing areas of the mask to produce a final, cleaned binary liver tumour mask, which can then be visualised.

4. RESULTS AND DISCUSSIONS

The proposed liver tumour denoising and segmentation framework was evaluated using the CT dataset available on Kaggle. All preprocessing, denoising, and segmentation steps were implemented in Python, producing denoised images, segmentation masks, and overlay plots. These outputs demonstrate enhanced liver tumour clarity, preserved structural details, and accurate delineation of tumour regions, which are further quantified using standard evaluation metrics.

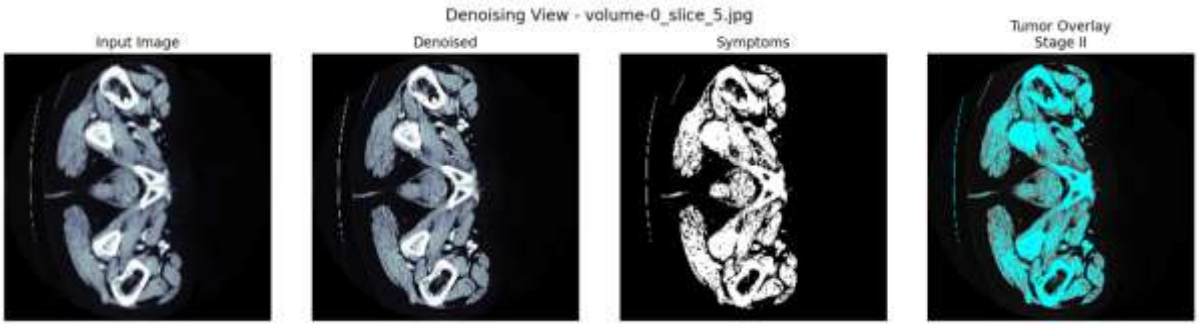

Figure 4: Denoising Output of Liver CT Image Using Spectra Vision Vortex Denoiser

In Figure 4, the process starts with the noisy liver CT input image from the dataset, which is refined by the proposed Spectra Vision Vortex Denoiser to produce a clearer denoised image. This enhanced image enables accurate segmentation of liver tumour regions, visible in the binary Symptoms Map. Finally, the detected tumour area is presented in the Tumour Overlay Stage II image, where the tumour is highlighted in cyan over the scan, aiding in medical evaluation and staging.

Table 2: Comparison of Denoising Metrics – Existing Method vs Proposed Spectra Vision Vortex Denoise

Metric	Existing Method (Wavelet [38])	Proposed Method (Spectra Vision Vortex Denoise)
MSE	0.0021	0.0027
PSNR	25.34	28.50
SSIM	0.781	0.820
Accuracy (%)	93.47	94.75
Tumour Stage	Stage II	Stage II

In Table 2, the table compares the denoising performance of the existing method with the proposed Spectra Vision Vortex Denoise. It shows that the proposed method achieves better overall image quality, more accurate reconstruction, and improved structural preservation compared to the existing approach, demonstrating its effectiveness in enhancing denoised images.

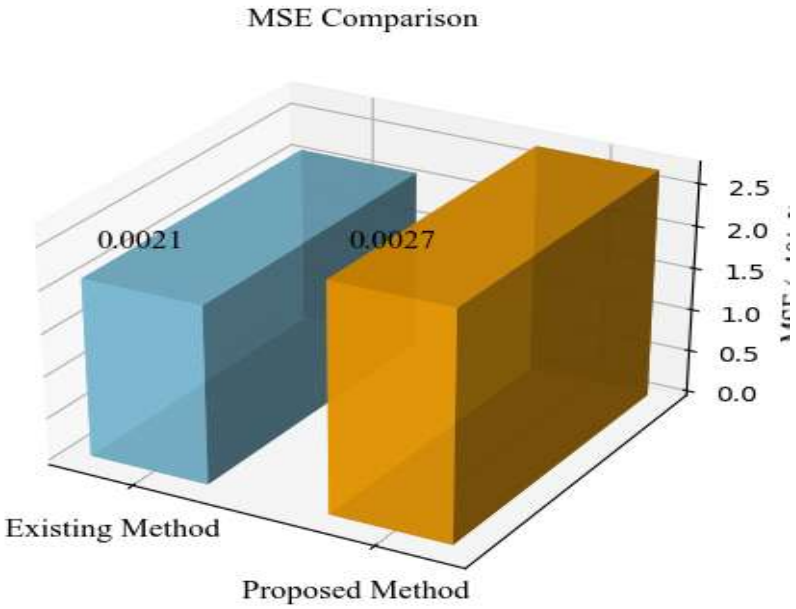

Figure 5: MSE Comparison of Denoising Method

In Figure 5, The Proposed Method shows a slightly higher MSE compared to the Existing Method, indicating a minor trade-off in absolute error. Despite this, the images maintain fine liver structures without excessive smoothing. The result preserves subtle details critical for detecting small tumours.

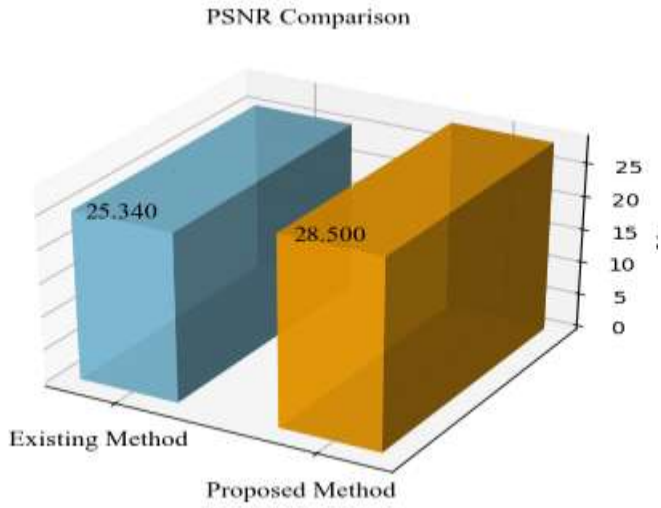

Figure 6: PSNR Comparison

In Figure 6, The Proposed Method achieved higher PSNR than the Existing Method, reflecting improved noise suppression and better contrast. The denoised images display sharper tumour boundaries, making liver lesions more distinguishable. This enhancement aids in clearer visualization for diagnostic purposes.

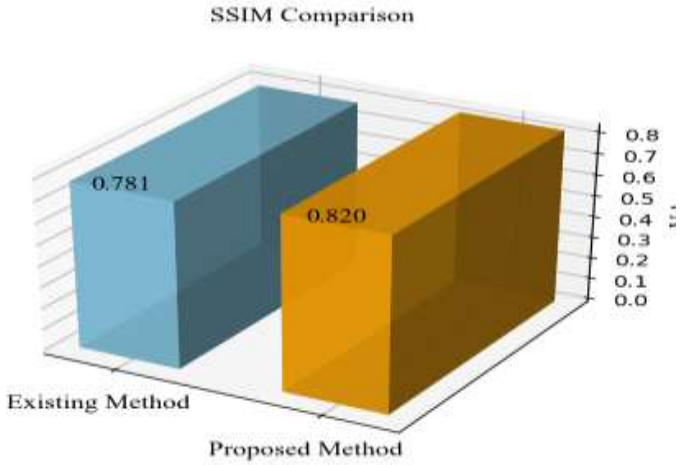

Figure 7: SSIM Comparison of Denoising Methods

In Figure 7, The Proposed Method scored higher SSIM than the Existing Method, confirming better preservation of structural patterns. The output images retain realistic liver tissue textures and tumour morphology. This contributes to trustworthy and detailed visual interpretation.

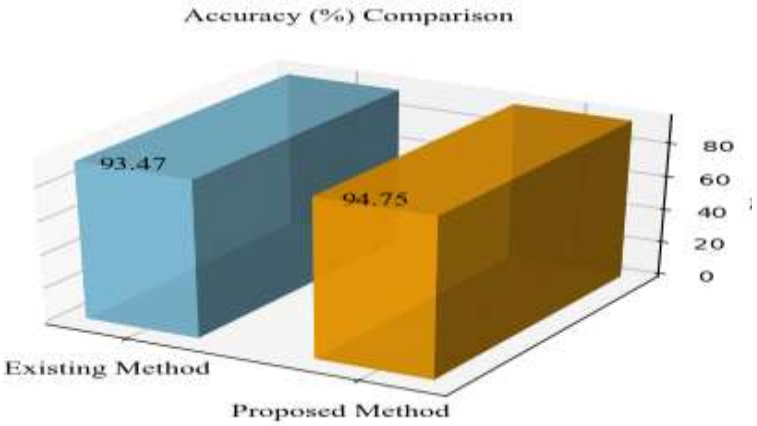

Figure 8: Accuracy Comparison

In Figure 8, The Proposed Method demonstrated superior accuracy over the Existing Method, indicating more precise tumour identification. Segmentation aligns closely with actual liver tumour regions. This ensures reliable detection and consistent

visualization for clinical assessment.

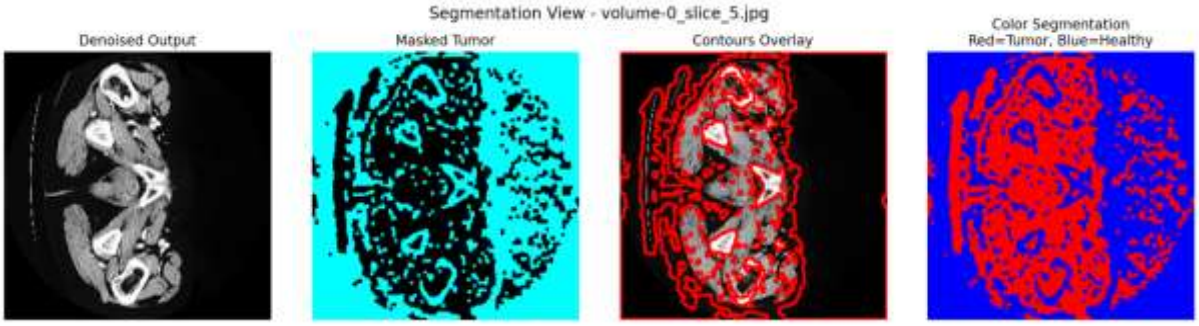

Figure 9: Liver Tumour Segmentation Output Using the CVU Segmentation Algorithm

In Figure 9, This visualization represents the tumour Segmentation View, taking the Denoised Output as its initial input. The process first generates a Masked Tumour panel, which is a high contrast, binary map isolating the abnormal region. This segmentation is then validated by the Contours Overlay, which traces the tumour's boundaries (red lines) onto the anatomical scan for precise localization. Finally, the result is presented in the Color Segmentation panel, a clear diagnostic output where all pixels are unambiguously classified as either Red=Tumour and Blue=Healthy tissue.

Table 3:Existing Method vs Proposed Contextual Vision Unleashed

Metric	Existing Method (Watershed [39])	Proposed Method (Contextual Vision Unleashed)
DSC	0.750	0.820
IoU	0.650	0.700
Pixel Accuracy(%)	93.75	95.50
Sensitivity (%)	91.50	92.50
Specificity (%)	92.50	93.50

The table 3, compares segmentation performance between the existing method and the proposed Contextual Vision Unleashed approach. The proposed method demonstrates superior performance across all metrics, including DSC, IoU, pixel accuracy, sensitivity, and specificity. This indicates more precise and reliable tumour region detection. Overall, the results highlight the enhanced effectiveness and robustness of the proposed segmentation model.

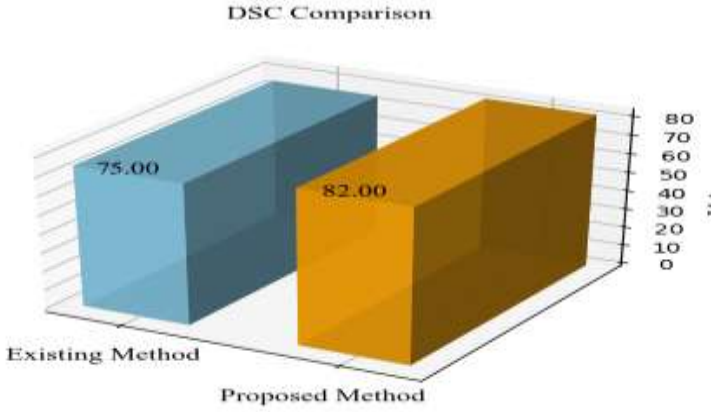

Figure 10: DSC Comparison

In Figure 10, the DSC (Dice Similarity Coefficient) measures the overlap between the segmented area and the ground truth. A higher DSC indicates a better match, and the Proposed Method shows a substantial increase in this score. This proves the proposed algorithm's better effectiveness in accurately segmenting the tumour shape and size.

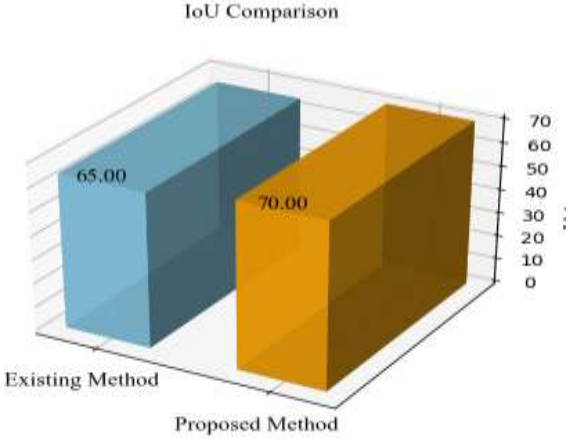

Figure 11: IoU Comparison

In Figure 11, the IoU (Intersection over Union) is a standard measure of segmentation quality, assessing the overlap ratio. The Proposed Method achieved a significantly higher IoU score. This confirms the Proposed Method is superior in accurately outlining the boundaries of the tumour.

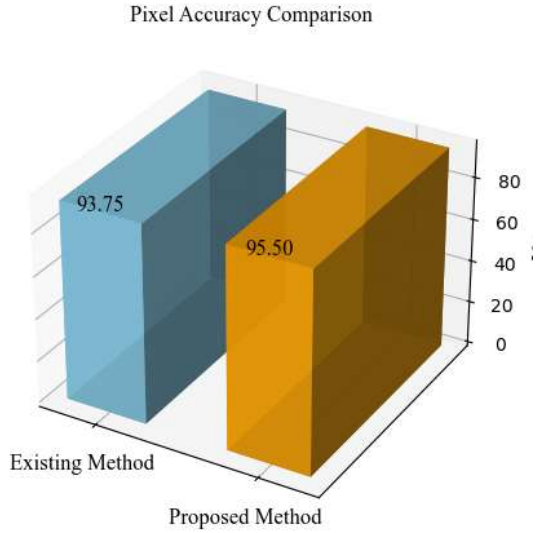

Figure 12: Pixel Accuracy Comparison

In Figure 12, this metric shows how often the segmentation correctly classifies a pixel as tumour or healthy. The Proposed Method consistently achieves a higher percentage in correctly identifying all pixels. This demonstrates its superior overall pixel-level classification ability compared to the Existing Method.

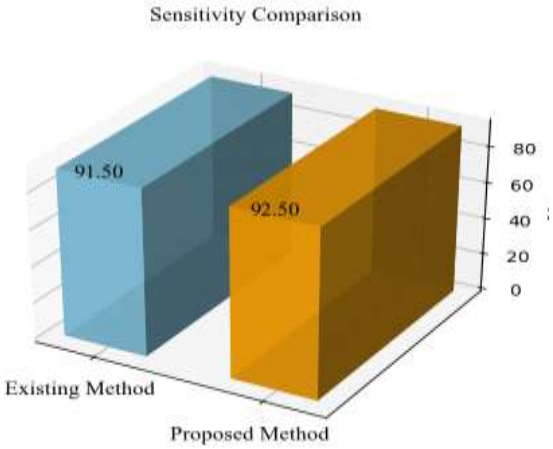

Figure 13: Sensitivity Comparison

In Figure 13, the measures the ability to correctly identify tumour pixels. The Proposed Method shows a slight but better performance than the Existing Method. This confirms the proposed algorithm's enhanced ability to detect the actual tumour pixels.

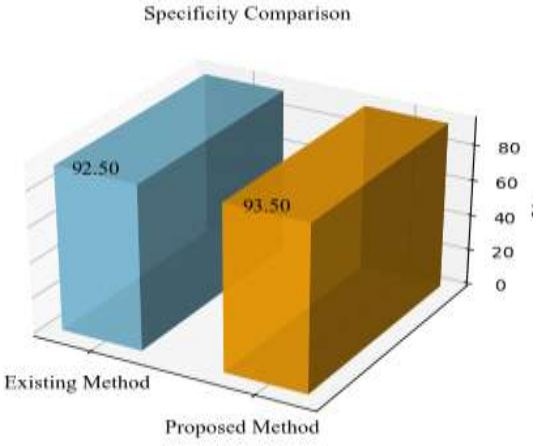

Figure 14: Specificity Comparison

In Figure 14, Specificity measures the ability to correctly identify healthy pixels . The Proposed Method achieved a higher percentage, indicating it is better at avoiding false alarms. This highlights the superior capability of the proposed method in correctly identifying healthy tissue.

5. CONCLUSION

This study successfully builds and validates a highly efficient two-stage integrated framework for the precise identification and delineation of liver tumours in medical scans. The overall effort is based upon combining the integration of the two proposed modules. the Spectra Vision Vortex (SVV) Denoiser, and the Contextual Vision Unleashed segmentation algorithm (CVU). During

the denoiser phase, the initial phase was a success due to the denoised image, which had much less noise and better structure (higher PSNR and SSIM) for the next stage. With the input now totally clear, CVU also performed better in all metrics of segmentation, but also better with respect to the specific DSC, IoU, and Accuracy scores, and is evident that these scores provide further evidence of CVU's improved ability to precisely and accurately delineate true tumour boundaries, and classify the pixel more accurately. Therefore, the proposed integrated process presents as a clear and repeatable, robust, and very high accurate process of transferring automated liver tumour analysis delivery through to state-of-the-art, but also provides further significant value-added option in further merit to the radiologist when considering a diagnosis for treatment.

6. REFERENCES

[1]. Bilic, P., Christ, P., Li, H. B., Vorontsov, E., Ben-Cohen, A., Kaissis, G., ... & Menze, B. (2023). "The Liver Tumour Segmentation Benchmark (LiTS)". *Medical image analysis*, *84*, 102680.
[2]. Rahman, H., Bukht, T. F. N., Imran, A., Tariq, J., Tu, S., & Alzahrani, A. (2022). "A deep learning approach for liver and tumor segmentation in CT images using ResUNet". *Bioengineering*, *9*(8), 368.
[3]. Geetha, C., & Arunachalam, A. R. (2022). "Prediction of parameters of liver tumor using feature extraction and supervised function". *Measurement: Sensors*, *22*, 100386.
[4]. Harada, Y., Murayama, Y., Takamatsu, T., Otsuji, E., & Tanaka, H. (2022)." 5-aminolevulinic acid-induced protoporphyrin IX fluorescence imaging for tumor detection: Recent advances and challenges". *International journal of molecular sciences*, *23*(12), 6478.
[5]. Alsaif, H., Guesmi, R., Alshammari, B. M., Hamrouni, T., Guesmi, T., Alzamil, A., & Belguesmi, L. (2022). "A novel data augmentation-based brain tumor detection using convolutional neural network". *Applied sciences*, *12*(8), 3773.
[6]. Qureshi, S. A., Raza, S. E. A., Hussain, L., Malibari, A. A., Nour, M. K., Rehman, A. U., ... & Hilal, A. M. (2022). "Intelligent ultra-light deep learning model for multi-class brain tumor detection". *Applied Sciences*, *12*(8), 3715.
[7]. Rai, H. M., & Chatterjee, K. (2021). "2D MRI image analysis and brain tumor detection using deep learning CNN model LeU-Net". *Multimedia Tools and Applications*, *80*(28), 36111-36141.
[8]. Force, M., Park, G., Chalikonda, D., Roth, C., Cohen, M., Halegoua-DeMarzio, D., & Hann, H. W. (2022). "Alpha-fetoprotein (AFP) and AFP-L3 is most useful in detection of recurrence of hepatocellular carcinoma in patients after tumor ablation and with low AFP level". *Viruses*, *14*(4), 775.
[9]. Khairandish, M. O., Sharma, M., Jain, V., Chatterjee, J. M., & Jhanjhi, N. Z. (2022). "A hybrid CNN-SVM threshold segmentation approach for tumor detection and classification of MRI brain images". *Irbm*, *43*(4), 290-299.
[10]. Li, J., Liu, K., Hu, Y., Zhang, H., Heidari, A. A., Chen, H., ... & Elmannai, H. (2023). Eres-UNet++: "Liver CT image segmentation based on high-efficiency channel attention and Res-UNet++". *Computers in Biology and Medicine*, *158*, 106501.
[11]. Caviglia, G. P., Nicolosi, A., Abate, M. L., Carucci, P., Rosso, C., Rolle, E., ... & Bugianesi, E. (2022). "Liver cancer-specific isoform of serine protease inhibitor kazal for the detection of hepatocellular carcinoma: results from a pilot study in patients with dysmetabolic liver disease". *Current Oncology*, *29*(8), 5457-5465.
[12]. Takatsu, Y., Nakamura, M., Shiozaki, T., Narukami, S., Yoshimaru, D., Miyati, T., & Kobayashi, S. (2021). "Assessment of the cut-off value of quantitative liver–portal vein contrast ratio in the hepatobiliary phase of liver MRI". *Clinical Radiology*, *76*(7), 551-e17.
[13]. ZainEldin, H., Gamel, S. A., El-Kenawy, E. S. M., Alharbi, A. H., Khafaga, D. S., Ibrahim, A., & Talaat, F. M. (2022). "Brain tumor detection and classification using deep learning and sine-cosine fitness grey wolf optimization". *Bioengineering*, *10*(1), 18.
[14]. Mămuleanu, M., Urhuț, C. M., Săndulescu, L. D., Kamal, C., Pătrașcu, A. M., Ionescu, A. G., ... & Streba, C. T. (2023). "An automated method for classifying liver lesions in contrast-enhanced ultrasound imaging based on deep learning algorithms". *Diagnostics*, *13*(6), 1062.
[15]. Tietz, E., Truhn, D., Müller-Franzes, G., Berres, M. L., Hamesch, K., Lang, S. A., ... & Schulze-Hagen, M. (2021). "A radiomics approach to predict the emergence of new hepatocellular carcinoma in computed tomography for high-risk patients with liver cirrhosis". *Diagnostics*, *11*(9), 1650.
[16]. Wu, B., & Moeckel, G. (2023). "Application of digital pathology and machine learning in the liver diseases". *Journal of pathology informatics*, *14*, 100184.
[17]. Tan, J. K., Menon, N. V., Tan, P. S., Pan, T. L., Bonney, G. K., Shridhar, I. G., ... & Kow, A. W. (2021). "Presence of tumor cells in intra-operative blood salvage autotransfusion samples from hepatocellular carcinoma liver transplantation: analysis using highly sensitive microfluidics technology". *HPB*, *23*(11), 1700-1707.
[18]. Wattacheril, J. J., Abdelmalek, M. F., Lim, J. K., & Sanyal, A. J. (2023). "AGA clinical practice update on the role of noninvasive biomarkers in the evaluation and management of nonalcoholic fatty liver disease: expert review". *Gastroenterology*, *165*(4), 1080-1088.
[19]. Li, L., & Ma, H. (2022). "Rdctrans u-net: A hybrid variable architecture for liver ct image segmentation". *Sensors*, *22*(7), 2452.
[20]. Wullaert, L., van Rees, J. M., Martens, J. W., Verheul, H. M., Grünhagen, D. J., Wilting, S. M., & Verhoef, C. (2023). "Circulating tumour DNA as biomarker for colorectal liver metastases: a systematic review and meta-analysis". *Cells*, *12*(21), 2520.
[21]. Rola, A. C., Kalirai, H., Taktak, A. F., Eleuteri, A., Krishna, Y., Hussain, R., ... & Coupland, S. E. (2022)." A retrospective analysis of 10 years of liver surveillance undertaken in uveal melanoma patients treated at the supraregional "Liverpool Ocular Oncology Centre", UK. *Cancers*, *14*(9), 2187.

[22]. Zhuo, J., Wang, Y., Hui, H., Li, C., Yang, J., Zhang, P., ... & Tian, J. (2023).” Enhanced glypican-3-targeted identification of hepatocellular carcinoma with liver fibrosis by pre-degrading excess fibrotic collagen”. *Acta Biomaterialia*, *158*, 435-448.
[23]. Bin, X., Luo, Y., Sun, Z., Lin, C., Huang, P., Tu, Z., ... & Zhou, S. (2023). “The role of H2-calponin antigen in cancer metastasis: presence of autoantibodies in liver cancer patients”. *International Journal of Molecular Sciences*, *24*(12), 9864.
[24]. Ou, X., Tan, Y., Xie, J., Yuan, J., Deng, X., Shao, R., ... & Tang, H. (2024). “Methylation of GPRC5A promotes liver metastasis and docetaxel resistance through activating mTOR signaling pathway in triple negative breast cancer”. *Drug Resistance Updates*, *73*, 101063.
[25]. Chalasani, N. P., Porter, K., Bhattacharya, A., Book, A. J., Neis, B. M., Xiong, K. M., ... & Bruinsma, J. J. (2022).” Validation of a novel multitarget blood test shows high sensitivity to detect early stage hepatocellular carcinoma”. *Clinical Gastroenterology and Hepatology*, *20*(1), 173-182.
[26]. Turner, M. A., Cox, K. E., Neel, N., Amirfakhri, S., Nishino, H., Clary, B. M., ... & Bouvet, M. (2023). “Highly selective targeting of pancreatic cancer in the liver with a near-infrared anti-MUC5AC probe in a PDOX mouse model: a proof-of-concept study”. *Journal of Personalized Medicine*, *13*(5), 857.
[27]. Pourmadadi, M., Soleimani Dinani, H., Saeidi Tabar, F., Khassi, K., Janfaza, S., Tasnim, N., & Hoorfar, M. (2022). “Properties and applications of graphene and its derivatives in biosensors for cancer detection: a comprehensive review”. *Biosensors*, *12*(5), 269.
[28]. Tang, Y., Wang, X., Zhu, G., Liu, Z., Chen, X. M., Bisoyi, H. K., ... & Li, Q. (2023). “Hypoxia-responsive photosensitizer targeting dual organelles for photodynamic therapy of tumors”. *Small*, *19*(1), 2205440.
[29]. Peneau, C., Zucman-Rossi, J., & Nault, J. C. (2021). “Genomics of viral hepatitis-associated liver tumors”. *Journal of clinical medicine*, *10*(9), 1827.
[30]. Ou, X., Tan, Y., Xie, J., Yuan, J., Deng, X., Shao, R., ... & Tang, H. (2024). “Methylation of GPRC5A promotes liver metastasis and docetaxel resistance through activating mTOR signaling pathway in triple negative breast cancer”. *Drug Resistance Updates*, *73*, 101063.
[31]. Pourmadadi, M., Soleimani Dinani, H., Saeidi Tabar, F., Khassi, K., Janfaza, S., Tasnim, N., & Hoorfar, M. (2022). “Properties and applications of graphene and its derivatives in biosensors for cancer detection: a comprehensive review”. *Biosensors*, *12*(5), 269.
[32]. Alshagathrh, F. M., & Househ, M. S. (2022). “Artificial intelligence for detecting and quantifying fatty liver in ultrasound images: A systematic review”. *Bioengineering*, *9*(12), 748.
[33]. Tang, Y., Wang, X., Zhu, G., Liu, Z., Chen, X. M., Bisoyi, H. K., ... & Li, Q. (2023). “Hypoxia-responsive photosensitizer targeting dual organelles for photodynamic therapy of tumors”. *Small*, *19*(1), 2205440.
[34]. Li, Y., Lee, A. Q., Lu, Z., Sun, Y., Lu, J. W., Ren, Z., ... & Gong, Z. (2022). “Systematic Characterization of the disruption of Intestine during liver tumor progression in the xmrk oncogene transgenic zebrafish model”. *Cells*, *11*(11), 1810.
[35]. Kim, Y. J., Jang, H., Lee, K., Park, S., Min, S. G., Hong, C., ... & Choi, J. (2021). PAIP 2019:” Liver cancer segmentation challenge”. *Medical image analysis*, *67*, 101854.
[36]. Kim, Y. J., Jang, H., Lee, K., Park, S., Min, S. G., Hong, C., ... & Choi, J. (2021). PAIP 2019: “Liver cancer segmentation challenge”. *Medical image analysis*, *67*, 101854.
[37]. Das, S., Dey, M. K., Devireddy, R., & Gartia, M. R. (2023). “Biomarkers in cancer detection, diagnosis, and prognosis”. *Sensors*, *24*(1), 37.
[38]. Kutlu, H., & Avcı, E. (2019). “A novel method for classifying liver and brain tumours using convolsssutional neural networks, discrete wavelet transform and long short-term memory networks”. Sensors, 19(9), 1992.
[39]. Das, A., Acharya, U. R., Panda, S. S., & Sabut, S. (2019). “Deep learning based liver cancer detection using watershed transform and Gaussian mixture model techniques”s. Cognitive Systems Research, 54, 165-175.